Grasping with PneuHand II

Mark E. Cambron
Department of Engineering
Western Kentucky University
Bowling Green, KY 42101
mark.cambron@wku.edu

Steven G. Northrup
Department of Electrical Engineering
Western New England College
Springfield, MA 01119
snorthru@wnec.edu

R. Alan Peters II
School of Engineering
Vanderbilt University
Nashville, TN 37212
rap2@vuse.vanderbilt.edu

***Abstract*— To interact with people in a human-centered environment a robot must exhibit intelligent behavior. This requires that the robot possess the ability to adapt its actions to changing environmental conditions. A robot estimates these conditions through sensing; therefore, intelligent behavior requires the ability to coordinate actions with the responses of sensors. That is, intelligent behavior requires sensory motor coordination (SMC). SMC is especially important in dexterous manipulation, which requires articulated arms and end-effectors. To test SMC related hypotheses, researchers at Vanderbilt University developed a simple pneumatic hand, which is described in this paper.**

***Index Terms*— Anthropomorphic Hand and Sensory Motor Coordination**

I. Introduction

In the past decade the field of service robots has emerged as an important research area. In 1996, Kawamura et al. [1] defined service robots as “reprogrammable, sensor-based mechatronic devices that perform useful service to human activities in an everyday environment.” Schraft [2], Kopacek et al. [3] and others have described the features that are required in service robots as follows: semi- or full automation, mobile and/or manipulation facilities, reliability and safety, and user friendly human-machine interaction.

High cost is one of the major reasons robots have not entered the main stream of society. Cost continues to hamper robot development at both Universities and Industry. End-effectors are particularly costly, so researchers at Vanderbilt designed the PneuHand to be an inexpensive device capable of simple distal-curl grasping.

The use of robots is limited by their lack of generality, which is especially apparent in end-effector design [4]. A general-purpose assistant robot would be required to work with a variety of objects. These objects would vary in size, weight, stiffness, fragility, etc. It is difficult to design one hand for all objects, hence a wide variety of robotic hands have been developed. Some are designed to grasp particular objects and are therefore unsuitable for grasping other objects. Many custom-designed end-effectors can only be used with one or two different objects. It has been estimated that such customized hands often represent 20 to 30 percent of the total robot system cost [4]. This limits robot flexibility in many industrial applications. The desire for more generally useful hands has lead researchers to design design end-effectors that resemble human hands [4], [5], [6], [7], [8], [9]. Many of these hands are expensive; it is possible to spend more on human-like robotic hands than for the rest of the robot.

The PneuHand is a low cost robotic hand with four fingers [10], [11] that was designed for human-like, distal-curl grasping. The design concept includes: manipulation of household objects and communication with humans via gestures.

To interact with people in a human-centered environment a robot must exhibit intelligent behavior. This requires that the robot possess the ability to adapt its actions to changing environmental conditions. A robot estimates these conditions sensing. Therefore, intelligent behavior requires the ability to coordinate actions with the responses of sensors. Intelligent behavior requires *sensory motor coordination* (SMC).

This paper reports a test of the hypothesis that a robot can acquire SMC with the PneuHand through repetitive control by a person. The learned SMC is then used for autonomous operation of the robot. If during repeated human-controlled trials of a task the robot records all of its sensory signals, then through statistical analysis, those sensory-motor couplings which accompany purposeful motion can be identified. As the trials are run, each necessarily under slightly different conditions, those sensory signals that reoccur in most trials are assumed to be significant to the task. Sensor signals that vary randomly are considered to be insignificant as far as the particular task is concerned. The SMC acquisition algorithm determines which parts of that information are significant and should be used, and which are insignificant and can be ignored. The significant information can be used to find exemplars of the SMC for the behaviors that comprise the task. Different exemplars then characterize different categories of tasks. During a subsequent autonomous execution of the task, the SMC information can be compared to the exemplars to determine the category of the robot-environment interaction.

II. Overview of a Humanoid Robot

Humanoid robots designed to assist human beings in human endeavors have requirements that differ significantly from those of industrial robots. Human safety under unpredictable conditions in a dynamic environment is primary in the design.

ISAC (Intelligent SoftArm Control) is an upper-torso humanoid with two 6-degree-of-freedom arms actuated pneumatically by McKibben Artificial Muscles (attached to the arms as antagonistic pairs) [12]. It’s end-effectors are the PneuHands. ISAC was developed at the Intelligent Robotics

Lab at Vanderbilt University as a test bed for human-robot interaction.

For a humanoid robot, safety demands, at the lowest level, that the robot arms be compliant, so that if they hit someone, the person will not be badly hurt. It also requires that control systems be fail-safe designed. That is, the robot must be designed to stop or to move out of the way whenever its sensors detect the potential for a person to be hurt [13].

ISAC provides a rich test bed for robot development due to the availability of many sensors and actuators and the relatively unstructured tasks for which it is used. For vision, the robot has has a color, stereo, active vision system with pan, tilt, and verge. The system implements the five basic oculomotor behaviors of primates: vergence, smooth pursuit, saccade, vestibular-ocular reflex, and opto-kinetic reflex [14]. The robot also employs sonic localization, infrared motion detection, and speech I/O. ISAC's control architecture is an agent-based, hybrid deliberative-reactive system. Like many behavior-based robots, ISAC's complex behaviors result from the interaction of independent computational modules that operate asynchronously in parallel [15].

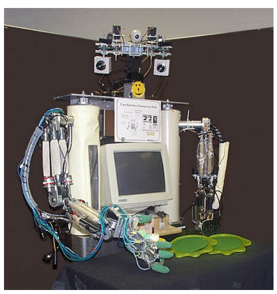

Fig. 1. Vanderbilt's Humanoid Robot: ISAC

III. ISAC'S ANTHROPOMORPHIC HANDS

Two versions of the low cost robotic hand, PneuHand I and PneuHand II, were developed for use with ISAC [10]. The designs were attempts to maximize functionality while minimizing cost, which is estimated to be under $2000. The hand was designed to be a natural part of the dual-armed humanoid, to be: anthropomorphic, light weight, and safe. PneuHand I consists of a central palm plate to which three fingers and an opposing thumb are connected [10], [11]. Each digit has

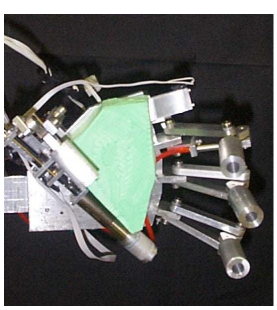

Fig. 2. Vanderbilt's PneuHand II

two phalanges and two joints, proximal and distal. Each digit is individually actuated by a pneumatic piston [16]. A PC add-on controller card, developed at Vanderbilt, controls the pneumatic valves [17]. Specifically, setting a desired pressure on the cylinder positions the finger in either an open or closed position.

The one actuator per digit design was intended to decrease the mass of the hand and to simplify its control; however, as a consequence of this, each digit of the PneuHand I has only two positions, opened or closed. The primary advantage of the PneuHand I over other simple grippers is its morphology. It has a human form factor and a distal curl closure that that enables it to grasp and to hold many objects (within the weight limits of the arm-hand system) that have a quasi-cylindrical handle (*e.g.* a telephone handset, a drinking glass, etc.) The PneuHand I can grasp with its thumb and one, two, or three fingers, but, it is does not have the dexterity to do things other than grasping and holding. The pneumatic servo system is not designed for slow and soft linear movement of the piston. Unfortunately, it tends to snap shut which can cause forces upon the object that displace the object in such a way to cause the grasp to fail.

The PneuHand II, shown in Figure 2, was designed to avoid the quick snap closure of the PneuHand I. To increase the controllability, a hybrid electric-pneumatic design was used. It has two motor actuators (in addition to the pistons), one each on the thumb and forefinger.

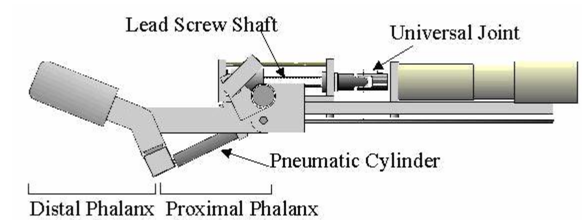

Fig. 3. PneuHand II Hybrid Finger [11]

Figure 3 shows the modification, a DC micro-motor connected to a lead screw by a universal joint [11]. The nut moves the drive link. These actuators give the thumb and forefinger a continuous range of positions between opened and closed. The finger retains a pneumatic cylinder for strength and an additional 1 DOF. In a typical grasp with the PneuHand II, the motors are used to close the thumb and forefinger on an object. Then the pistons are engaged to close the other two fingers and to add strength to the grasp of the thumb and forefinger.

Figure 4 shows the hardware controller circuit developed for the PneuHand II. The board has the following features:

- Controls the finger motors,
- Prevents the hand from moving past a safe point and burning out the DC finger motor,
- Shows the status of the limit switch,
- Shows the encoder reading, and
- Interfaces with the PC controller card [17].

The D flip-flop (SN74LS74) is used to disable the hand when a hardware limit is reached. The hand has 4 limit switches (2 for each motor) that signal when the hand has reached its hardware limit. A signal generated in software can override the disable signal. This is required in order to move the finger off the limit switch. The upper part of the circuit shows two Operational Amplifiers (L2722) and a voltage divider. The two Operational Amplifiers are used to control the motor that opens and closes the finger.

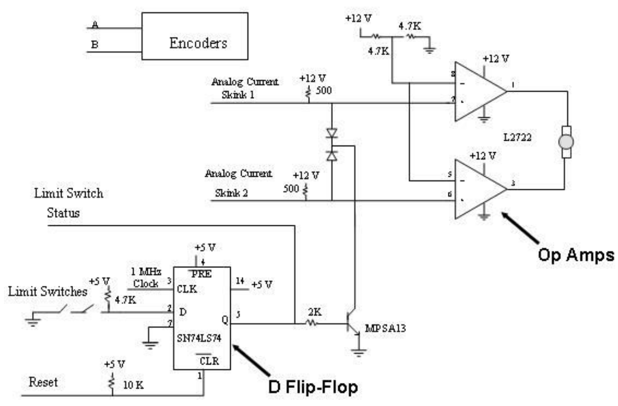

Fig. 4. PneuHand II Control Hardware

IV. Acquisition of SMC Parameters

One of the objectives of this work is to determine the SMC parameters which enable a robot to simultaneously perform a task and determine the category of the outcome. The SMC parameters are the motor action and concurrent sensory events that characterize the task. This work has been based on the hypothesis that these parameters must be acquired by the robot through experience; they cannot be preprogrammed. To enable parameter acquisition over a relatively short period of time, it was proposed for the user to operate the robot. The task would be performed a number of times via user control, covering the set of outcomes. From the sensory data collected during these trials, an autonomous control system would be defined.

The problem is limited to that of identifying a potentially incorrect grasp and letting the acquired signals determine, if necessary, a corrective step. In particular, the experiment entails the grasping of a stationary pole. The grasping problem requires the coordination of several behaviors that integrate multiple sensory and motor events. Experiments were conducted on two different types of stationary poles. The first pole was a cylindrical dowel. The second grasping experiment was conducted on rectangular pole.

Since the task has a set of different possible outcomes, this experiment requires definition of different categories of behavior external guidance for the robot through each trial. The robot can then use that data to create an autonomous control strategy and to distinguish the category of the outcome during subsequent grasp attempts.

Acquisition of SMC parameters entailed the following:

1) User controlled trials of the same task were run repeatedly with each of the possible outcomes represented equally. All sensory signals were recorded.
2) The signal set for each trial was partitioned (in time) into episodes by motor state changes, which served as temporal markers. For any given trial of the task the sensory signal is a multimodal vector denoted:

$$\vec{S}(t;r,p) = [\vec{S}_1(t;r,p) \quad \vec{S}_2(t;r,p) \cdots \vec{S}_M(t;r,p)] \qquad (1)$$

where subvector $\vec{S}_n(t;r,p)$ $(n = 1, \ldots, M)$ is the signal from sensor n, t is time, r is the trial number, and p is the episode number.[1]
3) For each episode, p, the signals from each trial, r, were resampled to normalize them in duration and sampling rate. Then for a specific p scalar signal $S_j(t;r,p)$ contained K_p samples in each trial, r. We assume that the number of samples exceeds the number of signals, that $K > N$.
4) Within episode p scalar signal $S_n((t;r,p))$ from a single sensor was compared across all trials. That is, the set

$$\{S_n((t;r,p))\}_{r=1}^{N} \qquad (2)$$

was analyzed for fixed p and fixed n across all trials, r. The analysis identified those sensors whose signals were similar in each trial. Those modalities were considered to be salient to the episode. Their signals were retained. Those sensors whose signals varied randomly across the trials were considered to be uninformative to the task during that episode; their signals were not considered further.
5) The retained signals were averaged across all trials. That is, within episode p, the scalar signals, $S_n((t;r,p))$ from sensor n (one for each trial, r) were averaged time-wise over r. The result was a set of characteristic signals $\chi_n(t;p)$, one for each relevant sensor and for each episode.

V. Pole Experiment

The objective of the two pole experiments was to enable ISAC to determine its wrist position relative to an object, in this case a stationary vertical pole just prior to grasping. The robot can then either close its grasp or if the hand is in the incorrect position, it can read just its position. During user control, sets of sensory data were collected while ISAC attempted to grasp the pole with the wrist set to one of three angles relative to the pole: $-10°$, $0°$ and $10°$. During the experiment sensory and motor signals are collected. The signals recorded are listed in Table I. During the grasping experiment vision is used to fixate upon an object, determine an initial location, and for the visual servoing algorithm. However, in the vast majority of the experiments the gripper and/or the target become occluded by the arm during grasp. During the final stages of the grasp the robot is blind. For this reason vision was not used in the final parts of the grasping operation.

[1] Some of the signals (*e.g.*, force) are vector-valued with multiple scalar components, while others (*e.g.*, proximity) have only one component. Nevertheless, the signal from sensor n is denoted by the vector $\vec{S}_n(t)$. Vector-valued signals have scalar signal components which are denoted S_j (without the arrow). There are M vector signals $\vec{S}_n(t)$ – one per sensor – and a total of N scalar signals S_j where $N > M$.

TABLE I

SIGNALS USED DURING USER CONTROL.

$\vec{S_1}$:	Arm positions (X,Y,Z,roll,pitch,yaw)
$\vec{S_2}$:	Finger Positions
$\vec{S_3}$:	6-axis Force-Torque sensor output
S_4:	Proximity sensor 1 output
S_5:	Proximity sensor 1 output
S_6:	Finger touch sensor 1
S_7:	Finger touch sensor 2
S_8:	Vision

Figure 5 is a composite graph of the sensor data in the 3 seconds before visual servoing algorithm was complete. The constant signals are the thumb and index finger position and the fingertip touch sensors, since the hand is open and not in contact with anything. The proximity sensors began firing during the final 2 seconds. The flattening of the signals dx, dy, and dz show that hand motion is slowing as the hand approaches the target location; therefore, the stability of the hand position and the firing of both proximity sensors are strong indicators that the hand has completed the servoing behavior and is in position to begin grasping.

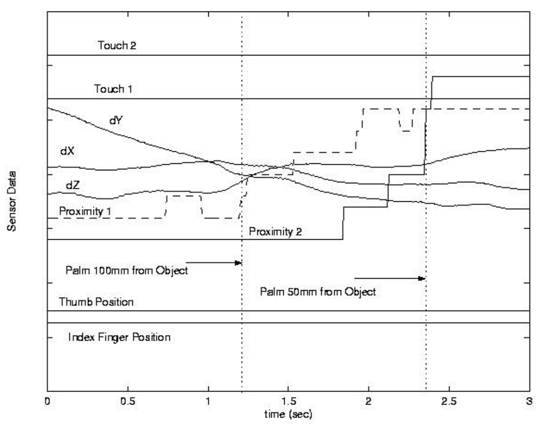

Fig. 5. Composite Sensors Data during one SMC episode

Figure 6 depicts the signals during the grasp procedure. In this figure, the signals indicate the positions of the fingers while closing, show when the touch sensors fire, and show the hand position stabilizing. Note that the proximity sensors continue to fire off and on as the hand moves toward the grasping position. This is due to the changing angle between the location of the sensor and the pole.

VI. LEARNING SMC

The motor control sequence within each trial was used to determine the motor events - - the times of transition between continuous motor operation states. The set of motor events from a trial were used to partition all the sensory signals within that trial into episodes. Given that researchers controlled the robot, there were the same number of motor events in each trial. Recall, that a *SMC event* is a motor state transition that is either preceded or followed by consistent signals in more than one sensor. During user control, this transition is initiated

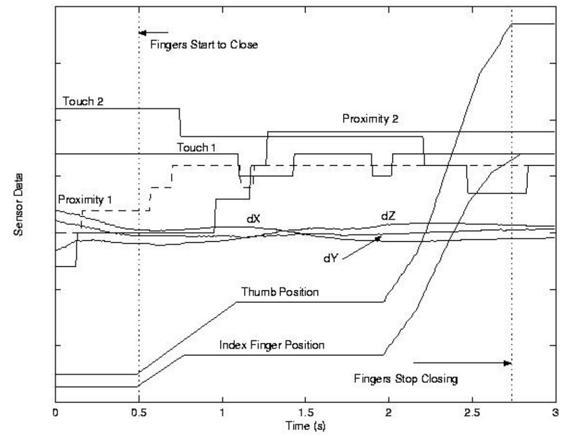

Fig. 6. Composite Sensors Data (Prior to end of Grasping)

by the operator; however, it is important to note that the time between these events (the episode durations) vary. Several of these motor events are shown in Figure 7. The force data recorded during a grasping experiment is plotted while the motor events are shown using vertical lines. Not only do the motor events indicate episode boundaries but also events from the sensory-motor data itself can be found. That is what the robot does during autonomous operation. For example, the time when the hand hits an object would be characterized by a significant change in total force, F_{total}, or total torque, F_{total}. The total force was found using the following:

$$F_{total}(t) = \sqrt{F_X(t)^2 + F_Y(t)^2 + F_Z(t)^2} \tag{3}$$

where $F_X(t)$, $F_Y(t)$, and $F_Z(t)$ are forces in the X, Y and Z directions. Force is measured with respect to relative position of the force torque sensor.

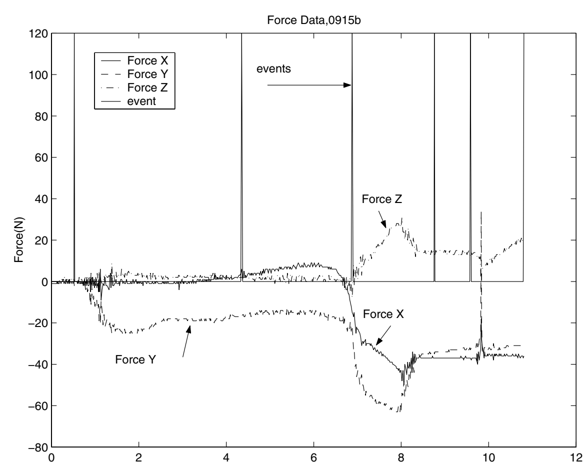

Fig. 7. Force Data and Events

In the experiment signals of 9 dimensions were used. The first 6 are composed of the force and torque data. During the grasping experiment, it was noted that the hand generally went slightly up (along the $\vec{z}$ axis) upon contact with the object; therefore, to measure the effect of this motion, a seventh motor signal (Δ_z) was added to the signal. In addition, the responses of the relative hand position in both the X (Δ_X) and $Y(\Delta_Y)$ directions were examined.

SMC requires the coupling of specific motor actions with specific sensory signals depending on the task context. There is a bootstrapping problem with this. Before the actions are performed, there is no way for the control system to know which subset of the signals to analyze, nor to know the events within those signals that are significant; therefore, acquiring SMC requires the robot to analyze all available sensory data and motor control information over the duration of the task. Within this analysis, significant events must be detected. The motor events as episode markers must be located within the data stream; then, the entire vector signal must be resampled to match the episode time intervals to previously acquired signals. To find the significant sensory-motor data, all the signals are processed. Once the SMC motor events are determined, the signals are resampled, filtered, and finally normalized.

The signals from the same episodes of the different trials undergo sampling-rate conversion so that they have the same sampling-rate and duration. The desired signal sampling rate is achieved through interpolation (up-sampling) by a factor, U, followed by decimating (down-sampling) the output of the interpolator by a factor, D. In other words, the sampling-rate conversion is accomplished by cascading an interpolator with a decimator. The length of signal is therefore converted from α by a rational factor U/D to a rate of β.

$$Rate = \frac{U}{D}\vec{S}_n(t;r,p) = \vec{S}_n(t;r,p) \tag{4}$$

After the signal is converted to the desired length, a simple 3-point running average filter was used to smooth the signal.

$$\vec{S}_{filter}(i) = \frac{\vec{S}(i)}{3} + \frac{\vec{S}(i-1)}{3} + \frac{\vec{S}(i-2)}{3} \tag{5}$$

where $\vec{Sig}$ is the signal and $\vec{Sig}_{filter}$ is the filter signal.

After R trials for each of the three hand angle outcomes $\theta \in \{0°, 10°, -10°\}$ were completed three characteristic signals $\vec{\chi}^{\,0}$, $\vec{\chi}^{\,10}$, and $\vec{\chi}^{\,-10}$ were computed. Each scalar component of these vector signals is then time-wise averaged over all trials with outcome θ of a given episode. For each outcome, θ, and each episode, p, let

$$\chi_n'^{\theta}(t;p) = \frac{1}{R}\sum_{r=1}^{R} S_n^{\theta}(t;r,p), \tag{6}$$

where each $S_n^{\theta}(t;r,p)$ was previously duration normalized. Each of these scalar characteristic signals is amplitude normalized with respect to its energy norm to get

$$\chi_n^{\theta}(t;p) = \frac{\chi_n'^{\theta}(t;p)}{\|\chi_n'^{\theta}(t;p)\|} \tag{7}$$

by taking the euclidian norm. The characteristic vector signal for outcome θ and episode p is then[2]

$$\vec{\chi}^{\,\theta}(t;p) = \left[\ \chi_1^{\theta}(t;p) \ \middle|\ \cdots \ \middle|\ \chi_N^{\theta}(t;p)\ \right] \tag{8}$$

[2]To distinguish between categories the superscript θ is used. When the statement is true for all categories no superscript is used.

VII. Experimental Results and Analysis

After the characteristic signals $\vec{\chi}^{\theta}(t;p)$ have been collected for each episode of the task, the robot was made to run autonomously using the learned SMC events to trigger motor changes and to determine the category of the outcome.

These signals collected during autonomous operation are hence referred to as the observed signal $\vec{S}(t;p)$. $\vec{S}(t;p)$ is the vector of N sensor signals from episode p (resampled and normalized). To facilitate the analysis the signal vector notation has been changed to a signal matrix notation.

For a given episode, p, the signal $\vec{S}$ contains K samples. $\vec{S}$ can be written as a K x N matrix where the row index corresponds to time and the column index to sensor modality. The observed signal is written in terms of its column vectors, then the signal matrix is:

$$\vec{S}(t;p) = [S_1(t;p) \quad S_2(t;p) \quad ... \quad S_n(t;p)] \tag{9}$$

We may write this as $\vec{S}(t)$ when the episode is implicit. When distinguishing between categories we use the superscript θ. When the statement is true for all categories we do not use the superscript. Each characteristic signal for episode p from outcome θ has a matrix of the same dimensions:

$$\vec{\chi}^{\theta}(t;p) = [\chi_1^{\theta}(t;p) \quad \chi_2^{\theta}(t;p) \quad ... \quad \chi_n^{\theta}(t;p)] \tag{10}$$

Both pole experiments had 3 possible outcomes. Several methods used to determine the category of the observed signal $\vec{S}(t;p)$ are described. Each of the sensor signals $S_N(t)$ lies in a K-dimensional space:

$$S_N \epsilon \Re^K \tag{11}$$

The N characteristic signals also lie in this space. Because $N < K$ the characteristic signals span a N-dimensional (or less) subspace of the K-dimensional signal space $\vec{S}(t;p)$. The idea is that each set of N characteristic vectors one for $-10°$, one for $0°$, and one for $10°$ forms a subspace in $\Re^K$, which may or may not include some vectors in with the other two.

The methods used to determine the category of the observed signal $\vec{S}(t;p)$ are given below.

Cross-Correlation at Time Lag 0: Cross-correlation at time lag 0 is a measure of how close the observed signal is to each of the three characteristic signals $\vec{\chi}^{-10}$, $\vec{\chi}^{0}$, and $\vec{\chi}^{10}$. For a given episode, p, the signals are resampled to the same duration and normalized to unit energy. A cross-correlation at time lag 0 is point by point test of similarity of each signal S_n with the corresponding characteristic signal χ_n for a given episode p. That is, each sensor signal S_n) is cross correlated with each characteristic signal $\vec{\chi}^{\theta}$ for each outcome θ.

Cross-Correlation with Non-Zero Time Lags: It is possible that the observed signal is slightly shifted in time (delayed or advanced) compared to the 3 characteristic signals. In order to study this situation we used a cross-correlation function that takes the time lag into consideration. This method is also a measure of similarity between the observed signal and the three characteristic signals, but the signals can also shifted in time.

Off-Diagonal Correlation Method at time lag 0: Another method of comparison using the results above was to take the difference between the autocorrelation matrices of each of the characteristic signals $\vec{\chi}^{\theta}$ and the correlation matrix between $\vec{S}$ and $\vec{\chi}^{\theta}$ (calculated using the cross-correlation at lag 0 method) This compares all possible signal correlations.

Singular Value Decomposition: The columns of each of the characteristic signals $\vec{\chi}^{\theta}$ matrix span a subspace of $\Re^K$, the signal space. If these subspaces are distinct then the projection of $\vec{S}$ onto each of them is a measure of the similarity of $\vec{S}$ to outcome θ. The singular value decomposition (SVD) method can be used to measure this type of similarity. The SVD for outcome θ describes the N-dimensional characteristic signal subspace (for outcome θ) in terms of an orthonormal basis set. The observed signal is projected on this subspace to measure the degree to which the observed signal lies in each characteristic signal subspace. The correlations methods also compare the observed signal to the different outcome subspaces, but more directly the cross-correlation is high only if the signals are similar. They could, in theory, lie in the same outcome subspace and be quite dissimilar. That case would result in a low correlation value, but a good fit from the SVD perspective.

Neural Network: Another method for used for category determination was a neural network. Neural networks are used to map inputs to categories. The network does this by partitioning the K-dimensional space into 3 subspaces each of which contains the N component characteristic signal for one outcome. This method has similar results to the correlation and SVD methods, but from a different prospective. This method does not directly compute characteristic signals, rather it uses the signals acquired via user control as exemplars for the training routine.

VIII. Results and Conclusions

The PneuHand design is modified to improve the grasping strategy of the humanoid robot. The issues in the first version of the hand have been discussed and the methodology of the redesigning has been presented. Sensory motor coordination was acquired by the robot through human-controlled training and several methods of signal classification. Testing was performed to determine the efficacy of five different methods used to determine the category of the observed signals. Table II shows results from these methods. The neural network method had classified the correct outcome with highest percentage (87.55%). However, the 3 correlation based methods all had similar results of 86.67% for the round pole. The rectangular pole showed a slight decrease for the off-diagonal correlation at time lag 0 method. Of the more effective methods, the Cross-Correlation at Time Lag 0 has the lowest computational expensive. The singular value decomposition method produced the poorest results of 73.33% and 66.67% for the round and rectangular poles. While the neural network gave the slightly better results, it is most computationally expensive of the algorithms. The neural network also needs to be retrained as new examples are created.

In conclusion, an inexpensive robotic hand on an upper torso humanoid robot has acquired SMC through human-controlled training. The robot is able to employ the sensory motor coordination to grasp two types of poles with an 87% success rate. The human-led training is a crucial to the robots ability to quickly attain the sensory motor coordination skills required to complete the task.

TABLE II

Summary of Classification Methods

Method	**Cyl. Pole**	**Rect. Pole**
Cross-Corr.(Time Lag 0)	86.67%	86.67%
Cross-Corr. with Non-Zero Time Lags	86.67%	86.67%
Off-Diagonal Corr. Method at time lag 0	86.67%	83.33%
Singular Value Decomposition	73.33%	66.67%
Neural Network (max)	87.55%	87.55%

Acknowledgment

The authors would like to thank members of the Center for Intelligent Systems past and present. Special acknowledgments are given to Mr. Joe Christopher and Dr. Kengo Ohnishi for their work in the mechanical design of the PneuHand.

References

[1] K. Kawamura, R. Pack, M. Bishay, and M. Iskarous, "Design philosophy for service robots," *Journal of Robotics and Autonomous Systems*, vol. 18, pp. 109–116, 1996.

[2] R. Schraft, "Mechatronics and robotics for service applications," *IEEE Robotics & Automation Magazine*, pp. 31–35, Dec. 1994.

[3] P. Kopacek and et al., "Modular service robotics - state of the art and future trends," in *Proceedings for ICAR'97*, pp. 51–56, 1997.

[4] J. Hollerback, "Workshop on the design and control of dexterous hands," Tech. Rep. AI Memo 661, MIT, Artificial Intelligence Laboratory, Cambridge, MA, 1982.

[5] S. Jacobsen, J. Wood, D. Knutti, and K. Biggers, "The utah/mit dextrous hand: Work in progress," *The International Journal of Robotics Research*, vol. 3, no. 4, pp. 21–50, 1984.

[6] C. Ruoff and J. Salisbury, "Multi-fingered robotic hand," Dec. 1984. U.S. Patent 4,921,293.

[7] K. Ohnishi, Y. Saito, T. Ihashi, and H. Ueno, "Human-type autonomous service robot arm: Haris," in *Proceedings of the 3rd France-Japan Congress & 1st Europe-Asia Congress on Mechatronics*, vol. 2, pp. 848–854, 1996.

[8] S. Hashimoto and et. al., "Hadaly-2 and wabian," in *Proceedings of IARP First International Workshop on Humanoid Friendly Robotics*, (Tsukuba, Japan), 1998.

[9] R. Ambrose and et al., "Robonaut: NASA's space humanoid," *IEEE Intelligent Systems*, vol. 15, pp. 57–63, July/August 2000.

[10] J. Christopher, "A pneuhand for human-like grasping on a humanoid robot," Master's thesis, Vanderbilt University, 1998.

[11] K. Ohnishi, M. Cambron, J. Christopher, and K. Nagata, "Report on the modifications on the pneuhand," tech. rep., Vanderbilt University, Intelligence Robotics Laboratory, Nashville, TN, May 1999.

[12] C. Chou and B. Hannaford, "Measurement and modeling of McKibben pneumatic artificial muscles," *IEEE Transactions on Robotics and Automation*, vol. 12, pp. 90–102, Feb. 1996.

[13] A. Kara, K. Kawamura, S. Bagchi, and M. El-Gamal, "Reflex control of a robotic aid system for the physically disabled," *IEEE Control Systems Magazine*, vol. 12, pp. 71–77, June 1992.

[14] A. Srikaew, *A Biologically Inspired Active Vision Gaze Controller*. PhD thesis, Vanderbilt University, Aug. 2000.

[15] R. Peters II, D. Wilkes, D. Gaines, and K. Kawamura, "A software agent based control system for human-robot interaction," in *Proceedings of 2^{nd} International Symposium on Humanoid Robotics*, (Tokyo, Japan), Oct. 1999.

[16] Robart Manufacturing, INC., "www.robart.com/." St. Charles, IL.

[17] S. Northrup, "A pc-based soft arm robot controller," Master's thesis, Vanderbilt University, 1997.